

Support effects on the atomic structure of ultrathin silica films on metals

Xin Yu, Bing Yang, Jorge Anibal Boscoboinik, Shamil Shaikhutdinov,^{a)}
and Hans-Joachim Freund

*Abteilung Chemische Physik, Fritz-Haber-Institut der Max-Planck-Gesellschaft, Faradayweg 4-6,
14195 Berlin, Germany*

(Received 13 February 2012; accepted 25 March 2012; published online 13 April 2012)

We studied the atomic structure of ultrathin silica films on Pt(111) in comparison with the previously studied films on Mo(112) and Ru(0001). The results obtained by scanning tunneling microscopy, photoelectron spectroscopy, and infrared reflection absorption spectroscopy suggest that the metal-oxygen bond strength plays the decisive role in the atomic structure of the silica overlayers on metal substrates. Metals with high oxygen adsorption energy favor the formation of the crystalline monolayer SiO_{2.5} films, whereas noble metals form primarily vitreous SiO₂ bilayer films. The metals with intermediate energies may form either of the structures or both coexisting. In the systems studied, the lattice mismatch plays only a minor role. © 2012 American Institute of Physics. [<http://dx.doi.org/10.1063/1.3703609>]

Many modern technological applications are based on silicon dioxide (SiO₂) thin layers. In addition, thin silica films grown on metal single crystal substrates are used as model systems for studying structure-property relationships of silica and related materials using surface science techniques.¹⁻⁵ One of the prominent examples in the literature relates to a crystalline silica film grown on Mo(112).^{2,6-10} It was shown that the ultrathin film consists of a single layer of corner sharing [SiO₄] tetrahedra forming a honeycomb-like network of a SiO_{2.5} stoichiometry, which is strongly bonded to Mo(112) through the Si-O-Mo linkages (the so-called “monolayer” silica film schematically shown in Fig. 1(a)).^{6,7} Recently, the preparation of SiO₂ films on Ru(0001) has been reported, where two layers of corner sharing [SiO₄] tetrahedra form a bilayer film that is weakly bonded to Ru(0001) (Fig. 1(b)).^{11,12} This structure resembles layered silicate minerals (diphylosilicates) and also the inner walls of some zeolites, e.g., MCM-41. More detailed studies, using x-ray photoelectron spectroscopy (XPS), infrared reflection absorption spectroscopy (IRAS), and scanning tunneling microscopy (STM) in combination with density functional theory calculations, showed that the silica films on Ru(0001) first grow as single monolayers, similar to that observed on Mo(112). The film transforms into the bilayer structure only with increase Si deposition.¹³ Depending on the preparation conditions, the bilayer film grows in either the crystalline or the vitreous state, or both coexist.^{11,13,14} Regardless of the substrate (Mo or Ru), thicker films grow only as vitreous silica, i.e., a three-dimensional random network of [SiO₄]. The principal structure of the films can be identified by IRAS, as each structure shows the individual vibrational band, i.e., ~1060 and ~1135 cm⁻¹ for monolayer films on Mo(112) and Ru(0001), respectively, reflecting the Si-O-Mo(Ru) linkages;^{6,13} ~1300 cm⁻¹ for the Si-O-Si linkages between the layers in the bilayer film on Ru(0001);¹¹ and ~1255 cm⁻¹ for the bulk-like vitreous silica films on various metal supports as well as Si crystals.^{1,13,15-17}

In order to understand the role of the metal support in the atomic structure of the ultrathin silica films, in this letter we studied the growth of silica films on Pt(111), for comparison with Mo(112) and Ru(0001). The Pt(111) surface has been widely used as a substrate for growing transition metal oxide thin films, e.g., titania, iron oxides, ceria, etc.¹⁸⁻²⁰ The surface exhibits the same symmetry, but has a slightly larger lattice constant than Ru(0001), i.e., 2.77 and 2.71 Å, respectively. In addition, the previously reported film preparations employed oxygen precovered metal surfaces prior to the Si deposition in the oxygen ambient. In this respect, Pt as the noble metal may behave differently than the Mo and Ru supports.

The experiments were performed in an UHV chamber (base pressure 5×10^{-10} mbar) equipped with LEED, XPS, IRAS, and STM. The Pt(111) crystal was mounted on the Omicron sample holder. The temperature was measured by a Type K thermocouple spot-welded to the edge of the crystal. The clean Pt(111) surface was obtained by cycles of Ar⁺ sputtering and annealing in UHV to 1273 K. The preparation of silica films on Pt(111) is nearly the same as that on

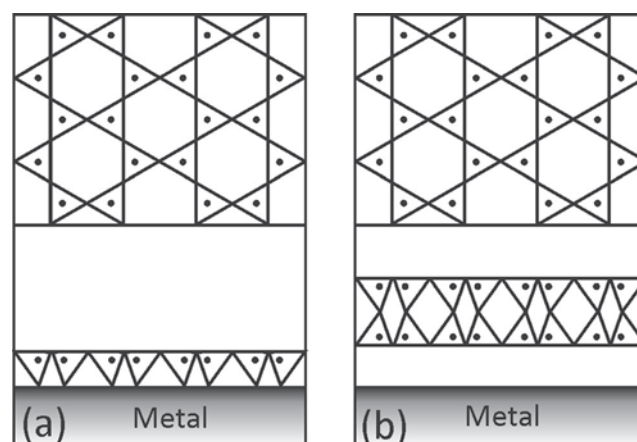


FIG. 1. Schematic representation of a monolayer (a) and a bilayer (b) film on a metal support. Top and cross views are shown. Si ion positions in [SiO₄] tetrahedra is indicated by dots.

^{a)}Author to whom correspondence should be addressed. Electronic mail: shaikhutdinov@fhi-berlin.mpg.de.

Ru(0001).^{11–14} First, we prepared the O-(2 × 2)-Pt(111) surface by exposing to 3×10^{-6} mbar O₂ at ~ 1200 K for 5 min and cooling to room temperature in the same ambient. Then Si (99.99%) was deposited using an e-beam assisted evaporator (EMT3, Omicron) in 1.5×10^{-6} mbar O₂ onto the substrate, which was kept at ~ 100 K. Final oxidation was performed in 1×10^{-5} mbar O₂ at ~ 1200 K. The amount of Si at the surface was measured by XPS using the well-established SiO_{2.5}/Mo(112) structure⁸ as a reference. For simplicity, the Si coverage is presented in the text in monolayer equivalents (MLE) such that 2 MLE corresponds to the amount of Si in the ideal bilayer film. The XPS spectra were referenced by setting the Au 4f_{7/2} level to 84.0 eV as measured on a clean gold foil.

First we address the structure of the 2 MLE silica films on Pt(111). The XPS measurements revealed only one chemical state of silicon, with a binding energy (BE) of the Si2p core level 102.8 eV that falls in the range of Si⁴⁺. For comparison, the value 102.5 eV was obtained for SiO₂/Ru(0001).^{11,12} The O1s region showed a main peak at 531.9 eV (531.7 eV for SiO₂/Ru(0001)) with a small shoulder at 530.1 eV contributing only $\sim 6\%$ to the overall signal intensity. The XPS data are very similar to those obtained for the bilayer film on Ru(0001), except that the ~ 530 eV shoulder is less prominent on Pt(111). The difference can, in principle, be assigned to the lower affinity of Pt(111) towards oxygen since this signal is associated with oxygen atoms directly adsorbed on the metal surface underneath a film¹² and/or in holes exposing a metal support.

The presence of small holes in this sample is seen in the large-scale STM image (Fig. 2(a)), which otherwise shows an uniformly covered film with relatively wide terraces separated by the monoatomic steps of Pt(111). The holes are ~ 2 Å in depth, which is considerably lower than the ~ 5 Å depth observed for the bilayer films on Ru(0001).^{13,14} On the other hand, the atomically resolved STM image shown in Fig. 2(b) is virtually identical to those obtained for the vitreous silica bilayer film on Ru(0001), where a random two-dimensional network of corner-sharing [SiO₄] tetrahedra results in a variety of N-membered rings, with N varying between 4 and 9.¹⁴ Also, LEED inspection showed only Pt(111) diffraction spots together with a diffuse (2 × 2) ring, thus indicating a lack of long-range ordering. In order to identify the principal structure of the film, one has to invoke IRAS since, as mentioned above, each silica structure exhibits individual vibrational bands.

The IRA-spectrum of this film, exhibiting only two sharp bands at 1294 and 690 cm⁻¹ (Fig. 3), is virtually identical to the one observed for the bilayer films on Ru(0001) (1302 and 692 cm⁻¹).¹¹ This finding straightforwardly leads to the conclusion that the film is bilayered in nature, and it grows in the vitreous state as judged by LEED and STM. Note that on Ru(0001) it was possible to grow crystalline films as well by using a low cooling rate after high temperature annealing.^{11,13,14} In the case of Pt(111), however, the crystalline films have not yet been observed at any combination of preparation parameters studied. This issue needs further studies and is beyond the scope of this paper.

Now we address the results for the 1 MLE films, which were prepared by reducing the amounts of Si deposited,

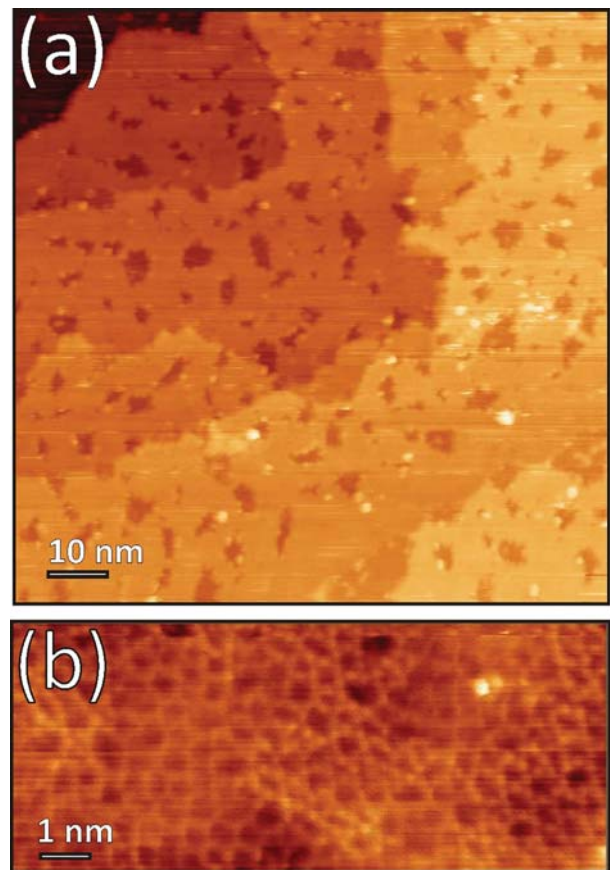


FIG. 2. Large-scale (a) and atomically resolved (b) STM images of the 2 MLE silica films on Pt(111). Tunneling parameters: bias 4.4 V and current 0.1 nA (a); 1.3 V, 0.13 nA (b).

while keeping all other parameters the same. The IRAS study immediately showed the bilayer structure of the resulting film (Fig. 3). It is clear that the intensity of the IRA bands at 1294 and 690 cm⁻¹ simply scales with the Si coverage and does not show any feature at 1000–1100 cm⁻¹ otherwise expected for a monolayer film. The scaling behavior is also observed in XP-spectra although the O/Pt(111) signal at

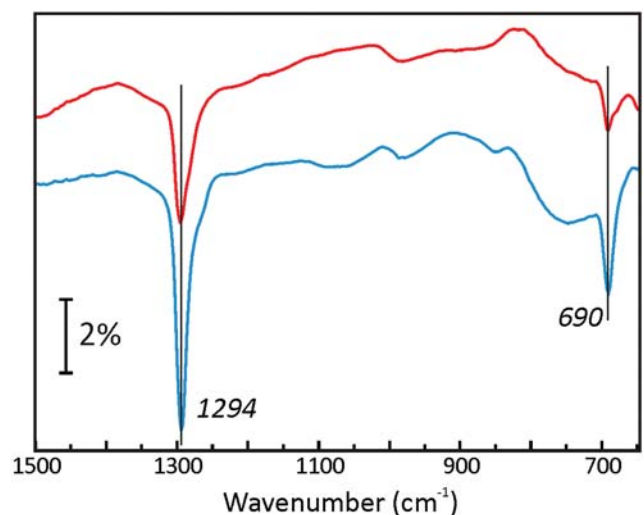


FIG. 3. IRA-spectra of 1 MLE (top) and 2 MLE (bottom) films grown on Pt(111).

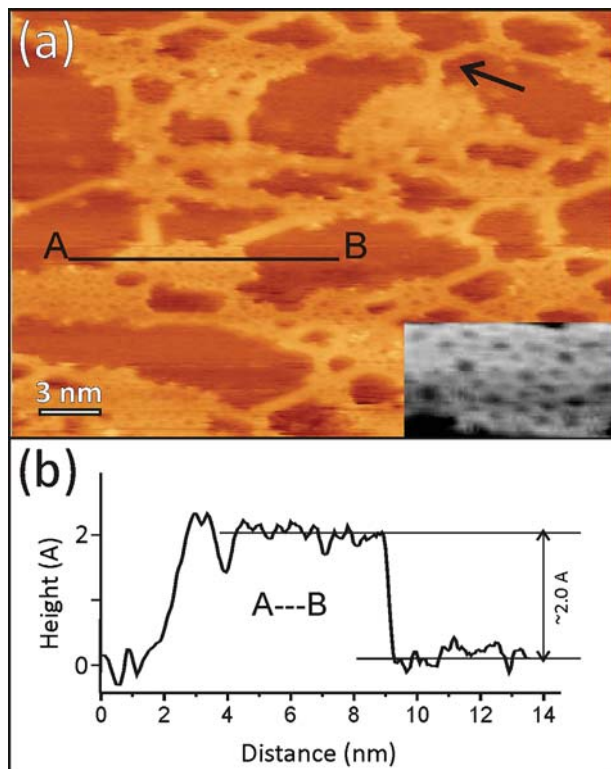


FIG. 4. (a) STM image of the 1 MLE film on Pt(111). Height profile along the A-B line, indicated in (a), is shown in (b). The inset shows a close-up image demonstrating the vitreous state of silica islands (cf., Fig. 2(b)). The arrow indicates silica stripes bridging the islands (tunneling parameters 0.8 V, 0.06 nA).

530 eV becomes more pronounced since the sample must expose larger fraction of the bare Pt surface.

Indeed, an STM image (Fig. 4) of the 1 MLE film shows that only half of the entire surface is covered by silica. The surface exposes two-dimensional islands, showing basically the same vitreous structure (zoomed in the inset in Fig. 4(a)) as in the case of the 2 MLE films (cf., Fig. 2(b)). The apparent height of the islands, i.e., in the order of 2 Å (Fig. 4(b)), is much lower than the geometrical film thickness, ~ 5 Å, but definitely higher than ~ 1.4 Å observed for the monolayer films on Ru(0001).¹³ Tentatively, we assign this behavior to the electronic effects frequently observed for STM imaging of metal-oxide systems, which, in addition, may be bias- and polarity-dependent. Interestingly, the islands are bridged by narrow stripes of the same height running primarily along the principal crystallographic directions of Pt(111). Most of these “bridges” are ~ 7 Å in width, although ~ 4 Å and ~ 10 Å wide lines were observed as well. To some extent, these stripes resemble one-dimensional silica rows formed at low Si coverage on Mo(112),²¹ although the atomic structure could not be identified here. Nonetheless, the above presented XPS, STM, and IRAS results show that ultrathin silica films on Pt(111) grow exclusively in the bilayer form.

Now we are in position to compare the principal structures of the ultrathin silica films grown on Mo(112), Ru(0001) and Pt(111). On all supports, the films are formed by a network of corner sharing $[\text{SiO}_4]$ tetrahedra. On Mo(112), silica grows only as a monolayer strongly bonded to Mo via the Si-O-Mo linkages. On Ru(0001), both monolayers, bonded through the Si-O-Ru linkage, and the bilayers,

weakly bonded to Ru, are observed, depending on the Si coverage. Irrespective of the Si coverage, only bilayer films grow on Pt(111). This trend correlates with the oxygen affinity to the metal support. Indeed, heats of dissociative adsorption of oxygen are of -544 , -220 , and -133 kJ/mole for Mo, Ru, and Pt, respectively,²² which correlate with standard heats of formation for MoO_2 , RuO_2 , and PtO_2 (-588 , -153 , and -71 kJ/mole, respectively).²³ Therefore, the SiO-Mo bond is much stronger than the SiO-Pt bond, and it will favor the monolayer structure, whereas on Pt silica forms “closed shell,” bilayer structure terminated by the fully saturated oxygen layer on either side. Ruthenium exhibits the intermediate properties and forms both mono- and bi-layer structures. Very recently, it has been reported the (accidental) formation of silica bilayer on graphene²⁴ that represents an oxygen-resistant, weakly bonded support. This finding is in full agreement with the trend observed above on metals.

One may argue that the lattice mismatch between an oxide film and a metal substrate, which is obviously different for the metals studied, may also play a role. The lattice constant of the unsupported, free-standing silica bilayer is computed to be 5.32 Å.⁹ When supported on Ru(0001) (lattice constant 2.71 Å) and Pt(111) (lattice constant 2.77 Å), the most natural structure for the silica film to accommodate these metal supports is the (2×2) structure resulting in a periodicity of 5.42 and 5.54 Å, respectively, that is indeed observed by LEED and STM. From this point of view, Ru(0001) is better suited than Pt(111) as the lattice mismatch is smaller. This may explain why on Ru(0001), and not on Pt(111), crystalline films may be grown under certain conditions.^{11,13} On the other hand, Mo(112) has a rectangular unit cell (5.46×8.92 Å) which hardly fit a hexagonal silica overlayer. As a result, the silica films on Mo(112) form the $c(2 \times 2)$ structure which is accompanied by a silica lattice extension along the Mo[-1-11] direction to 5.46 Å and a shortening along the Mo[-311] direction to 5.2 Å. However, despite this distortion, the monolayer silica film on Mo(112) is perfectly ordered on the large scale,^{6,8} whereas on Ru(0001) the monolayer film forms multi-domain structure with a high density of domain boundaries.¹³ Therefore, it is the strong SiO-Mo bond that stabilizes the well-ordered monolayer structure despite of the energy cost for the silica lattice distortion.

In summary, we studied the preparation and the atomic structure of ultrathin silica films on Pt(111) in comparison with the previously studied Mo(112) and Ru(0001). The results indicate that the metal-oxygen bond strength plays the decisive role in the atomic structure of silica overlayers on metal substrates. Metals with the high oxygen adsorption energy favor the formation of the crystalline monolayer $\text{SiO}_{2.5}$ films, whereas noble metals form primarily vitreous SiO_2 bilayer films. The metals with intermediate energies may form either of the structures or both coexisting. In the systems studied, the lattice mismatch plays only a minor role.

¹X. Xu and D. W. Goodman, *Appl. Phys. Lett.* **61**, 774 (1992).

²T. Schroeder, M. Adelt, B. Richter, M. Naschitzki, M. Bäumer, and H.-J. Freund, *Surf. Rev. Lett.* **7**, 7 (2000).

³M. S. Chen, A. K. Santra, and D. W. Goodman, *Phys. Rev. B* **69**, 155404 (2004).

⁴M. Kundu and Y. Murata, *Appl. Phys. Lett.* **80**, 1921 (2002).

- ⁵Z. Zhang, Z. Jiang, Y. Yao, D. Tan, Q. Fu, and X. Bao, *Thin Solid Films* **516**, 3741 (2008).
- ⁶J. Weissenrieder, S. Kaya, J.-L. Lu, H.-J. Gao, S. Shaikhutdinov, H.-J. Freund, M. M. Sierka, T. K. Todorova, and J. Sauer, *Phys. Rev. Lett.* **95**, 076103 (2005).
- ⁷L. Giordano, D. Ricci, G. Pacchioni, and P. Ugliendo, *Surf. Sci.* **584**, 225 (2005).
- ⁸S. Kaya, M. Baron, D. Stacchiola, J. Weissenrieder, S. Shaikhutdinov, T. K. Todorova, M. Sierka, J. Sauer, and H.-J. Freund, *Surf. Sci.* **601**, 4849 (2007).
- ⁹U. Martinez, L. Giordano, and G. Pacchioni, *J. Phys. Chem. B* **110**, 17015 (2006).
- ¹⁰J. Seifert, D. Blauth, and H. Winter, *Phys. Rev. Lett.* **103**, 017601 (2009).
- ¹¹D. Löffler, J. J. Uhlrich, M. Baron, B. Yang, X. Yu, L. Lichtenstein, L. Heinke, C. Büchner, M. Heyde, S. Shaikhutdinov, H.-J. Freund, R. Włodarczyk, M. Sierka, and J. Sauer, *Phys. Rev. Lett.* **105**, 146104 (2010).
- ¹²R. Włodarczyk, M. Sierka, J. Sauer, D. Löffler, J. J. Uhlrich, X. Yu, B. Yang, I. M. N. Groot, S. Shaikhutdinov, and H.-J. Freund, *Phys. Rev. B* **85**, 085403 (2012).
- ¹³B. Yang, X. Yu, J. A. Boscoboinik, L. Lichtenstein, M. Heyde, B. Kaden, R. Włodarczyk, M. Sierka, J. Sauer, S. Shaikhutdinov, and H.-J. Freund, “Thin silica films on Ru(0001): Monolayer, bilayer and three-dimensional networks of [SiO₄] tetrahedra,” (unpublished).
- ¹⁴L. Lichtenstein, C. Büchner, B. Yang, S. Shaikhutdinov, M. Heyde, M. Sierka, R. Włodarczyk, J. Sauer, and H.-J. Freund, *Angew. Chem. Int. Ed.* **51**, 404 (2012).
- ¹⁵J. E. Olsen and F. Shimura, *Appl. Phys. Lett.* **53**, 1934 (1988).
- ¹⁶K. T. Queeney, M. K. Weldon, J. P. Chang, Y. J. Chabal, A. B. Gurevich, J. Sapjeta, and R. L. Opila, *J. Appl. Phys.* **87**, 1322 (2000).
- ¹⁷D. J. Stacchiola, M. Baron, S. Kaya, J. Weissenrieder, S. Shaikhutdinov, and H.-J. Freund, *Appl. Phys. Lett.* **92**, 011911 (2008).
- ¹⁸P. Luches, F. Pagliuca, and S. Valeri, *J. Phys. Chem. C* **115**, 10718 (2011).
- ¹⁹W. Weiss and M. Ritter, *Phys. Rev. B* **59**, 5201 (1999).
- ²⁰U. Berner and K.-D. Schierbaum, *Phys. Rev. B* **65**, 235404 (2002).
- ²¹J. L. Lu, S. Kaya, J. Weissenrieder, T. K. Todorova, M. Sierka, J. Sauer, H. J. Gao, S. Shaikhutdinov, and H.-J. Freund, *Surf. Sci. Lett.* **600**, 164 (2006).
- ²²C. N. R. Rao, P. Vishnu Kamath, and S. Yashonath, *Chem. Phys. Lett.* **88**, 13 (1982).
- ²³B. A. Staskiewicz, J. R. Tucker, and P. E. Snyder, *J. Am. Chem. Soc.* **77**, 2987 (1955).
- ²⁴P. Y. Huang, S. Kurasch, A. Srivastava, V. Skakalova, J. Kotakoski, A. V. Krashennnikov, R. Hovden, Q. Mao, J. C. Meyer, J. Smet, D. A. Muller, and U. Kaiser, *Nano Lett.* **12**, 1081 (2012).